

A semi-analytical study for vibration analysis of damaged core laminated cylindrical shell with functionally graded CNTs reinforced face sheets resting on a two-parameter elastic foundation

Aseel J. Mohammed^{1a}, Bassam A. Mohammed^{2b}, Hatam K. Kadhom^{3c},
Anmar Ghanim Taki^{4d} and Vahid Tahouneh^{*5}

¹Department of Electromechanical Engineering, University of Technology-Iraq, Baghdad, Iraq

²Thermal Mechanic Techniques Engineering Department, Basra Engineering Technical College, Southern Technical University, Basra, Iraq

³Department of Electromechanical Engineering, University of Technology-Iraq, Baghdad, Iraq

⁴Department of Radiology Techniques, Health and Medical Techniques College, Alnoor University, Mosul, Iraq

⁵Young Researchers and Elite Club, Islamshahr Branch, Islamic Azad University, Islamshahr, Iran

(Received April 26, 2024, Revised September 12, 2024, Accepted September 13, 2024)

Abstract. The main objective of this paper is to study vibration of sandwich cylindrical shell with damaged core and FG face sheets resting on a two-parameter elastic foundation based on three-dimensional theory of elasticity. Three complicated equations of motion for the structure under consideration are semi-analytically solved by using generalized differential quadrature method. The structures are made of a damaged isotropic core and two external face sheets. These skins are strengthened at the nanoscale level by randomly oriented Carbon nanotubes (CNTs) and are reinforced at the microscale stage by oriented straight fibers. These reinforcing phases are included in a polymer matrix and a three-phase approach based on the Eshelby-Mori-Tanaka scheme and on the Halpin-Tsai approach, which is developed to compute the overall mechanical properties of the composite material. Several parametric analyses are carried out to investigate the mechanical behavior of these multi-layered structures depending on the damage features. A detailed parametric study is carried out in order to reveal the effects of different profiles of two-parameter elastic foundation modulus, different geometrical parameters such as the mid radius-to-thickness ratio, length-to-mean radius ratio and the thickness of face sheets on the vibrational characteristics of the damaged functionally graded sandwich cylindrical shell.

Keywords: damaged isotropic core; Eshelby-Mori-Tanaka scheme; generalized differential quadrature method; Halpin-Tsai equation; laminated cylindrical shell; three-dimensional theory of elasticity; two-parameter elastic foundation

1. Introduction

Usually sandwich structures consist of two outer layers, known as face sheets, and a lightweight core material in between, offering a high strength-to-weight ratio that makes them ideal for various applications. Widely used in aerospace for fuselage and wing designs, these structures also enhance vehicle performance in the automotive industry while reducing weight. The core can be made from materials like aluminum honeycomb, foam, or polymer composites, with face sheets typically crafted from carbon fiber, glass fiber, or metals. Their ability to resist bending and buckling, along with energy absorption capabilities, makes them suitable for safety applications. In construction, sandwich panels provide excellent thermal insulation, while in marine applications, they reduce the weight of boats and

ships without compromising structural integrity. Manufacturing processes such as lamination, molding, and extrusion are employed, often optimized through finite element analysis, enabling tailored designs for specific performance criteria. Furthermore, they improve acoustic performance, making them valuable in soundproofing applications, and are utilized in wind turbine blades and rail transportation for lightweight designs. However, recycling sandwich materials poses challenges, though advances in materials science are underway. Functionally graded sandwich structures (FGSS) take this concept further by featuring a gradual variation in material properties across layers, optimizing mechanical and thermal performance. This gradation minimizes stress concentration and improves load distribution, finding applications in high-temperature environments like turbine blades and in biomedical engineering for implants that mimic natural bone properties. Advanced manufacturing techniques, including 3D printing, enable the creation of FGSS, which enhance fatigue resistance and can exhibit tailored electrical properties for electronic applications. Their multi-functional capabilities simplify designs by reducing the number of components in a system and are increasingly researched for applications in civil engineering, such as bridge reinforcement. Optimization of FGSS can lead to significant cost savings, and the

*Corresponding author, Ph.D.,

E-mail: vahid.th1982@gmail.com

^a Ph. D., E-mail: Aseel.j.Mohammed@uotechnology.edu.iq

^b Ph. D., E-mail: bassam.moh@stu.edu.iq

^c Ph. D., E-mail: hatam.k.kadhom@uotechnology.edu.iq

^d Ph. D., E-mail: anmar.ghanim@alnoor.edu.iq

environmental impact can be mitigated by using sustainable materials. As research continues, the development of sandwich structures and FGSS represents a significant advancement in material science and engineering, paving the way for next-generation applications across various industries.

Due to the mismatch of stiffness properties between the face sheets and the core, sandwich plates and panels are susceptible to face sheet/core debonding, which is a major problem in sandwich construction, especially under impact loading (Abrate 1998). Various material profiles through the functionally graded plate and panel thickness can be illustrated by using parameter power-law distribution. In fact, by considering power-law distribution, it is possible to study the influence of different kinds of material profiles. Abouelregal and Marin (2020a) studied The Size-Dependent Thermoelastic Vibrations of Nanobeams Subjected to Harmonic Excitation and Rectified Sine Wave Heating. A nonlocal thermoelastic model that illustrates the vibrations of nanobeams is introduced. Based on the nonlocal elasticity theory proposed by Eringen and generalized thermo elasticity, the equations that govern the nonlocal nanobeams are derived. The structure of the nanobeam is under a harmonic external force and temperature change in the form of rectified sine wave heating. The nonlocal model includes the nonlocal parameter (length-scale) that can have the effect of the small-scale. In another study (Zhang *et al.* 2022) the nanofluid, composed of kerosene and tantalum and nickel nanoparticles, is propagating through a porous, elastic surface. The kerosene base fluid is incompressible and electrically conducting. In another study (Amari *et al.* 2023), the authors consider the resistance of the radially-graded graphene-platelets reinforced (RG-GPLR) nanocomposite annular sector plates against thermal shock. For the first time, this study considers the effect of thermal shock induced by the radical temperature gradient, heat flux, and the mixed form. Recently, Viola and Tornabene (2009) used three-parameter power-law distribution to study the dynamic behavior of functionally graded parabolic panels of revolution. Though there are research works reported on general sandwich structures, very little work has been done to consider the vibration behavior and static response of FGM structures (Anderson 2003, Kashtalyan and Menshykova 2009, Barka *et al.* 2016, Chen *et al.* 2017, Tornabene *et al.* 2016a, b). Fantuzzi *et al.* (2016) used Non-Uniform Rational B-Spline (NURBS) curves to describe arbitrary shapes with holes and discontinuities. By means of above-mentioned method, they have analyzed free vibration of arbitrarily shaped FG carbon nanotube-reinforced plates. Brischetto *et al.* (2015) studied free vibration of simply supported Single- and Double-Walled Carbon Nanotubes (SWCNTs and DWCNTs). A continuum approach (based on an elastic three-dimensional shell model) was used for natural frequency investigation of SWCNTs and DWCNTs. SWCNTs were defined as isotropic cylinders with an equivalent thickness and Young modulus. DWCNTs were defined as two concentric isotropic cylinders (with an equivalent thickness and Young modulus). Li *et al.* (2008) studied free vibrations of FG sandwich rectangular plates with simply supported and clamped edges. Zenkour (2005a,

b) presented a two-dimensional solution to study the bending, buckling and free vibration of simply supported FG ceramic-metal sandwich plates. Kamarian *et al.* (2013) studied free vibration of FGSW rectangular plates with simply supported edges and rested on elastic foundations using differential quadratic method. The natural frequencies of FGM circular cylindrical shells were investigated by Loy *et al.* (1999), which was later extended to cylindrical shells under various end supporting conditions (Pradhan *et al.* 2000). Patel *et al.* (2005) carried out the vibration analysis of functionally graded shell using a higher-order theory. Pradyumna *et al.* (2008) studied the free vibrations analysis of functionally graded curved panels via a higher-order finite element formulation. Free vibration and dynamic instability of FGM cylindrical panels under combined static and periodic axial forces were studied by using a proposed semi-analytical approach (Yang and Shen 2003). Elastic response analysis of simply supported FGM cylindrical shell under low-velocity impact was presented by Gang *et al.* (1999). Vibrations and wave propagation velocity in a functionally graded hollow cylinder were studied by Shakeri *et al.* (2006). They assumed that the shell to be in plane strain condition and subjected to an axisymmetric dynamic loading. The free vibration of simply supported, fluid-filled cylindrically orthotropic functionally graded cylindrical shells with arbitrary thickness was investigated by Chen *et al.* (2004). Recently, Tornabene (2009) used four-parameter power-law distribution to study the dynamic behavior of moderately thick functionally graded conical and cylindrical shells. In his study, the two-constituent functionally graded isotropic shell was consisted of ceramic and metal, and the generalized differential quadrature method was used to discretize the governing equations. Tahouneh *et al.* (2020a) considered vibration analysis of vacancy defected graphene sheet as a nonisotropic structure via molecular dynamic and continuum approaches. In another study (Tahouneh *et al.* 2020b) the vibration analysis of a single-layered graphene sheet (SLGS) with corner cutout based on the nonlocal elasticity model framework of classical Kirchhoff thin plate was investigated. Paliwal *et al.* (1995 and 1996) have investigated the free vibration of whole buried cylindrical shells with simply supported ends in contact with Winkler and Pasternak foundations using direct solution to the governing classical shell theory equations of motion. Bouguenina *et al.* (2015) studied FG plates with variable thickness subjected to thermal buckling. Wu and Liu (2016) developed a state space differential reproducing kernel (DRK) method in order to study 3D analysis of FG circular plates. Park *et al.* (2016) used modified couple stress based third-order shear deformation theory for dynamic analysis of sigmoid functionally graded materials (S-FGM) plates. Yang *et al.* (1998) have investigated the behavior of whole buried pipelines subjected to sinusoidal seismic waves by the finite element method. Bouafia *et al.* (2021) studied Natural frequencies of FGM nanoplates embedded in an elastic medium. Khadir *et al.* (2021) investigated buckling and free vibration of functionally graded carbon nanotubes reinforced composite laminated nanoplates. The frequency characteristics, and sensitivity analysis of a size-dependent laminated composite

cylindrical nanoshell under bi-directional thermal loading using Nonlocal Strain-stress Gradient Theory (NSGT) was studied by Dai *et al.* (2021). In another study, Ebrahimi *et al.* (2019) studied the frequency response of curved magneto-electro-viscoelastic functionally graded (CMEV-FG) nanobeams. Boutaleb *et al.* (2019) studied the dynamic response of the functionally graded rectangular nanoplates. The theory of nonlocal elasticity based on the quasi 3D high shear deformation theory (quasi 3D HSDT) has been employed to determine the natural frequencies of the nanosize FG plate. Free vibration and stability of functionally graded shallow shells according to a 2-D higher order deformation theory were investigated by Matsunaga (2008). Civalek (2005) investigated the nonlinear dynamic response of doubly curved shallow shells resting on Winkler–Pasternak elastic foundations using the harmonic differential quadrature (HDQ) and finite differences (FD) methods. Hong and Lee (2015) presented a spectral element model for a modified FGM axial bar model wherein non-uniform lateral contraction in the thickness direction was taken into account.

Othman and Marin (2017) studied the wave propagation of generalized thermoelastic medium with voids under the effect of thermal loading due to laser pulse with energy dissipation. The material was a homogeneous isotropic elastic half-space and heated by a non-Gaussian laser beam with the pulse duration of 0.2 ps. A normal mode method was proposed to analyse the problem and obtain numerical solutions for the displacement components, stresses, temperature distribution and the change in the volume fraction field. Marin and Öchsner (2017) investigated the mixed initial boundary value problem for a dipolar body in the context of the thermoelastic theory proposed by Green and Naghdi. For the solutions of this problem they proved a result of Hölder's-type stability on the supply terms. They considered middle restrictions on the thermoelastic coefficients, which were common in continuum mechanics. For the same conditions they proposed a continuous dependence result with regard to the initial data. Abouelregal and Marin (2020b) considered nonlocal nanobeams analysis depending on the theories of Euler-Bernoulli and modified couple-stress (MCS). It also was assumed that the thermal conductivity of the nanobeam was dependent on the temperature. Physical fields of the nanobeam were obtained utilizing Laplace transform and state-space techniques. The effects of the size and nonlocal parameters, variability of thermal conductivity and couple stress on various distributions were presented graphically and studied in detail. Arefi (2015) suggested an analytical solution of a curved beam with different shapes made of functionally graded materials (FGMs). Bennai *et al.* (2015) developed a new refined hyperbolic shear and normal deformation beam theory to study the free vibration and buckling of functionally graded (FG) sandwich beams under various boundary conditions. Bouchafa *et al.* (2015) used refined hyperbolic shear deformation theory (RHSDT) for the thermoelastic bending analysis of functionally graded sandwich plates. Moradi-Dastjerdi and Momeni-Khabisi (2016) studied free and forced vibration of plates reinforced by wavy carbon nanotube. The plates were

resting on Winkler-Pasternak elastic foundations and subjected to periodic or impact loading. In another investigation, CNT/epoxy nanocomposite have been fabricated by in situ polymerization technique and piezoresistive responses of the samples have been recorded and evaluated (Afrookhteh *et al.* 2016). The 3D microstructure of the gas diffusion layers (GDLs) was generated, using a stochastic reconstruction approach. The method used basic input parameters and fibers orientation distribution and was capable to model carbon fiber and binder phases of all types of carbon fiber GDLs with different structural parameters (Afrookhteh *et al.* 2016). Zhang and Wang (2020) studied the effects of Van der Waals force on the vibration of Multi-layered nanostructures. Wang and Hu (2014) investigated thermal vibration of SWCNTs with quantum effects using the models of Euler and Timoshenko beam theories. Jam *et al.* (2017) studied the nonlinear free vibration analysis of micro-beams resting on the viscoelastic foundation. Hosseini and Zhang (2018) considered wave propagation analysis in an FG Graphene platelets-reinforced nanocomposite cylinder.

Nowadays, the use of carbon nanotubes in polymer/carbon nanotube composites has attracted the attention of many researchers (Wagner *et al.* 1997). A high aspect ratio, low weight of CNTs, and their extraordinary mechanical properties (strength and flexibility) provide the ultimate reinforcement for the next generation of extremely lightweight but highly elastic and very strong advanced composite materials. On the other hand, by using of the polymer/CNT composites in advanced composite materials, we can achieve structures with low weight, high strength and high stiffness in many structures of civil, mechanical and space engineering. In structural mechanics, one of the most popular semi-analytical methods is differential quadrature method (DQM) (Bellman and Casti 1971, Tahouneh 2014, 2016, Tahouneh and Naei 2014), remarkable success of which has been demonstrated by many researchers in vibration analysis of plates, shells, and beams. Tornabene *et al.* (2014) studied free vibration of free-form doubly-curved shells made of functionally graded materials using higher-order equivalent single layer theories. The partial differential system of equations was solved by using the Generalized Differential Quadrature (GDQ) method. The recent developments of the differential quadrature method as well as its major applications in engineering are discussed in detail in the book by Shu (2000). To the best of the authors' knowledge, no papers have been reported in the literature concerning the vibrational behavior of damaged core laminated cylindrical shells with FG sheets resting on a two-parameter elastic foundation and finite length. In this study, the structures are made of a damaged isotropic core and two external face sheets. These skins are strengthened at the nanoscale level by randomly oriented Carbon nanotubes (CNTs) and are reinforced at the microscale stage by oriented straight fibers. These reinforcing phases are included in a polymer matrix and a three-phase approach based on the Eshelby-Mori-Tanaka scheme and on the Halpin-Tsai approach, which is developed to compute the overall mechanical properties of the composite material. Using GDQ method,

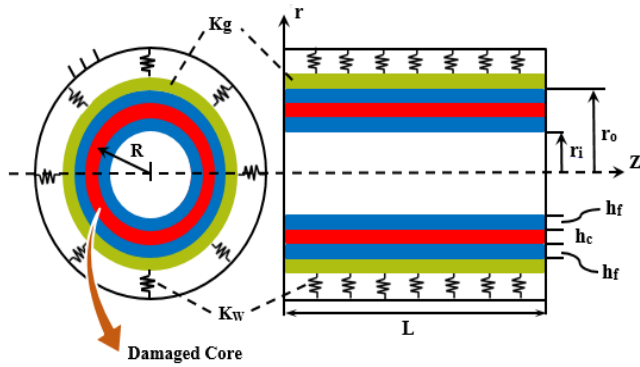


Fig. 1 Geometry and coordinates of the thick sandwich cylindrical shell with Damaged Core and Face Sheets

the free vibration analysis of three-layer sandwich cylindrical shells with the damaged core is investigated and natural frequencies of the structures are obtained.

2. Geometric and mechanical characterization

Consider a thick FG damaged core sandwich cylindrical shell rested on elastic foundations as shown in Fig. 1. The length, mean radius, uniform thickness, the thickness of face sheets, and inner and outer radius of the shell are L , R , H , h , r_i , and r_o , respectively. The outer surface of the shell is continuously in contact with an elastic medium that acts as an elastic foundation represented by the Winkler/ Pasternak model with Winkler stiffness k_w and shearing layer stiffness k_g . It should be specified that a perfect bonding is assumed between two adjacent layers in the proposed model.

2.1 Mechanical properties of the face sheets

A multiscale approach is employed to evaluate the overall mechanical properties of the three phase composite face-sheets (Tornabene *et al.* 2019, Bacciocchi and Tarantino 2019). These layers are made of fiber-reinforced materials, which means that a polymer matrix (epoxy resin) is strengthened by oriented straight fibers (Carbon fibers). The third constituent is given by randomly oriented Carbon nanotubes (CNTs), which are inserted in the matrix and are used to further increase its mechanical features. The overall properties are computed by means of a two-step approach. Firstly, the Eshelby-Mori-Tanaka scheme is applied to obtain the properties of the epoxy resin including CNTs (Eshelby 1957, Mori and Tanaka 1973). At this stage, the composite turns out to be isotropic due to the fact that the nanoparticles are randomly oriented, as illustrated in the paper by Shi *et al.* (2004). Then, the Halpin-Tsai approach is applied to combine the features of the enriched matrix with the properties of the reinforcing straight fibers (Halpin 1969, Tsai 1964 and Tsai 1965). At the nano-scale level, the single fiber of CNT is modeled as a linear-elastic, transversely isotropic and homogeneous cylindrical solid, as proposed in the paper by Odegard *et al.* (2003). Its mechanical properties are described by five parameters,

which are the Hill's elastic moduli (Hill 1964a, b), defined as k_c , l_c , m_c , n_c , p_c . Its density ρ_c is required to compute the volume fraction of CNTs V_c as follows:

$$V_c = \left(\frac{\rho_c}{\omega_c \rho_M} - \frac{\rho_c}{\rho_M} + 1 \right)^{-1} \quad (1)$$

where ρ_M represents the density of the polymer matrix, whereas ω_c stands for the mass fraction of CNTs. A uniform distribution of CNTs is assumed in each layer along the thickness direction. It should be recalled that the matrix volume fraction is given by $V_M = 1 - V_C$. The polymer matrix is isotropic, and it is fully characterized by its Young's modulus E_M and Poisson's ratio ν_M . In the following, its bulk modulus K_M and shear modulus G_M are required in order to apply the Eshelby-Mori-Tanaka approach (Eshelby 1957, Mori and Tanaka 1973). The following definitions are needed for this purpose

$$K_M = \frac{E_M}{3(1 - 2\nu_M)}, \quad G_M = \frac{E_M}{2(1 + \nu_M)} \quad (2)$$

These quantities are noticeably affected by the presence of randomly oriented CNTs. As illustrated in the paper by Shi *et al.* (2004), if the agglomeration of CNTs is neglected, the bulk modulus K_M^* and the shear modulus G_M^* of the enriched matrix are given by:

$$K_M^* = K_M + \frac{V_c(\delta_c - 3K_M\alpha_c)}{3(V_M + V_c\alpha_c)}, \quad (3)$$

$$G_M^* = G_M + \frac{V_c(\eta_c - 2G_M\beta_c)}{2(V_M + V_c\beta_c)}$$

where the following quantities, which can be computed by defining the Hill's elastic moduli of CNTs, are introduced:

$$\alpha_c = \frac{3(K_M + G_M) + k_c + l_c}{3(G_M + k_c)},$$

$$\beta_c = \frac{1}{5} \left(\frac{4G_M + 2k_c + l_c}{3(G_M + k_c)} + \frac{4G_M}{G_M + P_c} + \frac{2(G_M(6K_M + 8G_M))}{G_M(3K_M + G_M)m_c(3K_M + 7G_M)} \right), \quad (4)$$

$$\delta_c = \frac{1}{3} \left(n_c + 2l_c + \frac{(2k_c + l_c)(3K_M + G_M - l_c)}{G_M + k_c} \right),$$

$$\eta_c = \frac{1}{5} \left(\frac{2}{3}(n_c - l_c) + \frac{8G_M P_c}{G_M + P_c} + \frac{2(k_c - l_c)(2G_M + l_c)}{3(G_M + k_c)} + \frac{8m_c G_M(3K_M + 4G_M)}{3K_M(m_c + G_M) + G_{PM}(7m_c + G_M)} \right).$$

Finally, the evaluation of K_M^* and G_M^* allows to compute the Young's modulus E_M^* and the Poisson's ratio ν_M^* of the polymer matrix enriched by CNTs:

$$E_M^* = \frac{9K_M^* G_M^*}{3K_M^* + G_M^*}, \quad \nu_M^* = \frac{3K_M^* - 2G_M^*}{6K_M^* + 2G_M^*} \quad (5)$$

whereas its density is given by:

$$\rho_M^* = (\rho_c - \rho_M) V_c + \rho_M \quad (6)$$

The mechanical properties of a single CNT fiber in terms of its Hill's elastic moduli, as well as its density, are listed in Table 1. Such properties are valid for a single-

walled Carbon nanotube with 10 as chiral index and armchair structure. Further details about the mechanical characterization of CNT can be found in (Tornabene *et al.* 2019).

In order to apply the Halpin-Tsai approach that allows to compute the overall mechanical properties of the composite given by this enriched matrix including straight Carbon fibers, the Hill's elastic moduli of the matrix k_M^* , l_M^* , m_M^* , n_M^* , p_M^* are needed. For this purpose, the following definitions are introduced:

$$k_M^* = \frac{E_M^*}{2(1+\nu_M^*)(1-2\nu_M^*)}, \quad l_M^* = 2\nu_M^*k_M^*, \quad m_M^* = (1-2\nu_M^*)k_M^* \quad (7)$$

$$n_M^* = 2(1-\nu_M^*)k_M^*, \quad p_M^* = (1-2\nu_M^*)k_M^*$$

Analogously, the Hill's elastic moduli of the Carbon fibers k_F , l_F , m_F , n_F , p_F are required. The reinforcing fibers are assumed as transversely isotropic and their mechanical properties are given by the corresponding Young's moduli E_{11}^F , E_{22}^F , shear modulus G_{12}^F and Poisson's ratios ν_{12}^F , ν_{23}^F . Once these quantities are known, the Hill's elastic moduli can be easily evaluated:

$$k_F = \frac{E_{22}^F}{2(1-\nu_{23}^F-2\nu_{21}^F\nu_{12}^F)},$$

$$l_F = 2\nu_{12}^Fk_F, \quad m_F = \frac{1-\nu_{23}^F-2\nu_{21}^F\nu_{12}^F}{1+\nu_{23}^F}k_F, \quad (8)$$

$$n_F = 2(1-\nu_{23}^F)\frac{E_{11}^F}{E_{22}^F}k_F, \quad p_F = G_{12}^F$$

As shown in the previous step, the density of the fibers ρ_F is required to compute the reference value of the corresponding volume fraction V_F^* , once their mass fraction ω_F is defined

$$V_F^* = \left(\frac{\rho_F}{\omega_F\rho_M^*} - \frac{\rho_F}{\rho_M^*} + 1 \right) \quad (9)$$

Consequently, the volume fraction distribution of the fibers V_F is given by $V_F = \bar{V}_F * V_F^*$ and it is clearly non-uniform along the thickness of the face sheets. The definitions of \bar{V}_F is specified bellow (Kamarian *et al.* 2013)

$$\bar{V}_f = \begin{cases} 1 - \left\{ \left(\frac{-(r-R) + 0.5\hbar}{\hbar_f} \right) + b \left(1 - \frac{-(r-R) + 0.5\hbar}{\hbar_f} \right)^c \right\}^p, & 0.5\hbar - \hbar_f \leq r-R \leq 0.5\hbar \\ 0, & -0.5\hbar + \hbar_f \leq r-R \leq 0.5\hbar - \hbar_f \\ 1 - \left\{ \left(\frac{(r-R) + 0.5\hbar}{\hbar_f} \right) + b \left(1 - \frac{(r-R) + 0.5\hbar}{\hbar_f} \right)^c \right\}^p, & -0.5\hbar \leq r-R \leq -0.5\hbar + \hbar_f \end{cases} \quad (10)$$

where the parameter p ($0 \leq p < \infty$) and the parameters b and c dictate the fiber variation profile through the radial direction of the sandwich panel. The through-thickness variations of the \bar{V}_F of the sandwich panel are shown in Figs. 2-5.

At this point, the Halpin-Tsai approach can be applied to obtain the Hill's elastic moduli of the composite layers, which are denoted by k , l , m , n , p :

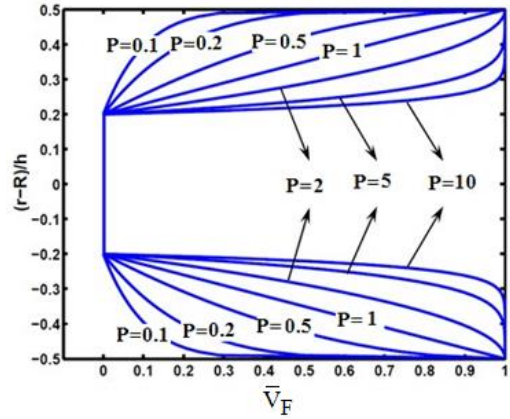


Fig. 2 Variation of the \bar{V}_F through the thickness of the FG graded sheets ($b=0$, $c=2$)

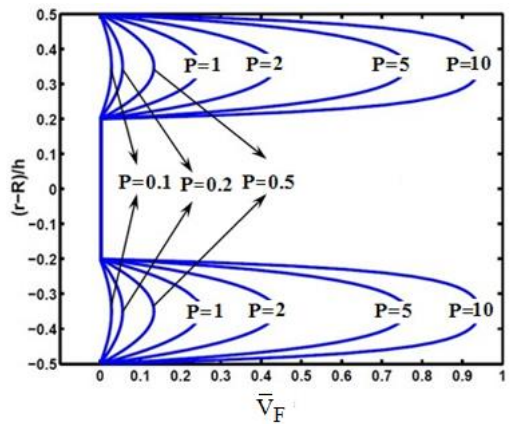


Fig. 3 Variation of the \bar{V}_F through the thickness of the FG graded sheets ($b=1$, $c=2$)

$$k = \frac{k_M^*(k_F + m_M^*)V_M^* + k_F(k_M^* + m_M^*)V_F}{(k_F + m_M^*)V_M^* + (k_M^* + m_M^*)V_F},$$

$$l = V_F l_F + V_M^* l_M^* + \frac{l_F - l_M^*}{k_F - k_M^*} (k - V_F k_F - V_M^* k_M^*),$$

$$m = m_M^* \frac{2V_F m_F (k_M^* + m_M^*) + 2V_M^* m_F m_M^* + V_M^* k_M^* (m_F + m_M^*)}{2V_F m_M^* (k_M^* + m_M^*) + 2V_M^* m_F m_M^* + V_M^* k_M^* (m_F + m_M^*)} \quad (11)$$

$$n = V_F n_F + V_M^* n_M^* + \left(\frac{l_F - l_M^*}{k_F - k_M^*} \right)^2 (k - V_F k_F - V_M^* k_M^*),$$

$$p = \frac{(p_F + p_M^*)p_M^* V_M^* + 2p_F p_M^* V_F}{(p_F + p_M^*)V_M^* + 2p_M^* V_F}$$

being $V_M^* = 1 - V_F$. The engineering constants of these layers can be evaluated according to the following definitions:

$$E_{11} = n - \frac{l^2}{k}, \quad E_{22} = \frac{4m(kn - l^2)}{kn - l^2 + mn}, \quad \nu_{12} = \frac{l}{2k}, \quad (12)$$

$$G_{12} = G_{13} = p, \quad G_{23} = m$$

Finally, the density of the composite face-sheets is given by:

$$\rho = (\rho_F - \rho_M^*)V_F + \rho_M^* \quad (13)$$

In the following, the same constituents are used in the

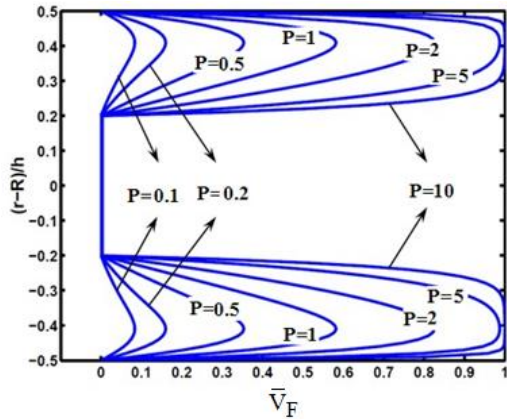


Fig. 4 Variation of the \bar{V}_F through the thickness of the FG graded sheets ($b=1, c=6$)

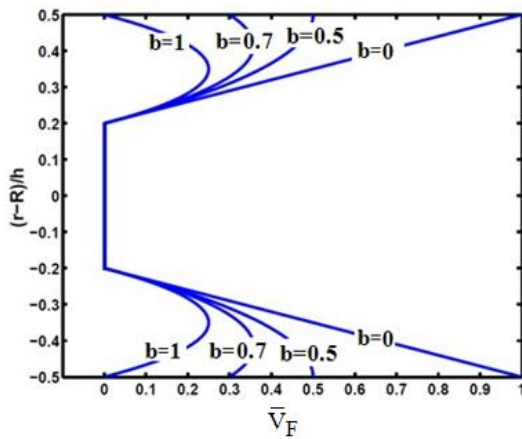


Fig. 5 Variation of the \bar{V}_F through the thickness of the FG graded sheets ($c=2$)

Table 2 Mechanical properties of the layer constituents

Constituent	Young's Moduli	Shear Moduli	Poisson's Ratios	Density
Carbon fibers	$E_{11}^F=230$ GPa	$G_{12}^F=50$	$\nu_{12}^F=0.20$	$\rho_F=1800$ kg/m ³
	$E_{22}^F=15$ GPa		$\nu_{23}^F=0.25$	
Epoxy resin	$E_M=3.27$ GPa	-	$\nu_M=0.38$	$\rho_M=1200$ kg/m ³

external layers assuming also the same values of the mass fractions of both CNTs and fibers.

2.2 Mechanical properties of the damaged matrix

The core of the sandwich structures considered in the paper made of the same polymer matrix used in the face-sheets. Nevertheless, a damage model is introduced to provide an analytical description of an irreversible rheological process that causes the decay of the mechanical properties, in terms of engineering constants. An isotropic damage is considered in the following, which is fully characterized by a scalar D as illustrated in the book by Lemaitre and Chaboche (1990). The elastic modulus of the damaged material is given by:

$$E = (1 - D)E_M \tag{14}$$

in which E_M is the original value of matrix Young's modulus, for $0 \leq D < 1$. It is clear that $D=0$ identifies a virgin material, whereas a fully damaged material is characterized by $D=1$. For conciseness purposes, the mechanical properties of the undamaged epoxy resin and the Carbon fibers are summarized in Table 2.

3. Governing equations

The mechanical constitutive relation that relates the stresses to the strains are as follows:

$$\begin{Bmatrix} \sigma_z \\ \sigma_\theta \\ \sigma_r \\ \tau_{r\theta} \\ \tau_{zr} \\ \tau_{z\theta} \end{Bmatrix} = \begin{bmatrix} \bar{C}_{11} & \bar{C}_{12} & \bar{C}_{13} & 0 & 0 & 0 \\ \bar{C}_{21} & \bar{C}_{22} & \bar{C}_{23} & 0 & 0 & 0 \\ \bar{C}_{31} & \bar{C}_{32} & \bar{C}_{33} & 0 & 0 & 0 \\ 0 & 0 & 0 & \bar{C}_{44} & 0 & 0 \\ 0 & 0 & 0 & 0 & \bar{C}_{55} & 0 \\ 0 & 0 & 0 & 0 & 0 & \bar{C}_{66} \end{bmatrix} \begin{Bmatrix} \varepsilon_z \\ \varepsilon_\theta \\ \varepsilon_r \\ \gamma_{r\theta} \\ \gamma_{zr} \\ \gamma_{z\theta} \end{Bmatrix} \tag{15}$$

In the absence of body forces, the governing equations are as the following (Sobhani Aragh and Yas 2010):

$$\begin{aligned} \frac{\partial \sigma_z}{\partial z} + \frac{\partial \tau_{z\theta}}{r \partial \theta} + \frac{\partial \tau_{rz}}{\partial r} + \frac{\tau_{rz}}{r} &= \rho \frac{\partial^2 u_z}{\partial t^2}, \\ \frac{\partial \tau_{\theta z}}{\partial z} + \frac{\partial \sigma_\theta}{r \partial \theta} + \frac{\partial \tau_{r\theta}}{\partial r} + \frac{2\tau_{r\theta}}{r} &= \rho \frac{\partial^2 u_\theta}{\partial t^2}, \\ \frac{\partial \tau_{zr}}{\partial z} + \frac{\partial \tau_{\theta r}}{r \partial \theta} + \frac{\partial \sigma_r}{\partial r} + \frac{\sigma_r - \sigma_\theta}{r} &= \rho \frac{\partial^2 u_r}{\partial t^2} \end{aligned} \tag{16}$$

Strain-displacement relations are expressed as:

$$\begin{aligned} \varepsilon_r &= \frac{\partial u_r}{\partial r}, \varepsilon_\theta = \frac{u_r}{r} + \frac{1}{r} \frac{\partial u_\theta}{\partial \theta}, \varepsilon_z = \frac{\partial u_z}{\partial z}, \\ \gamma_{z\theta} &= \frac{\partial u_\theta}{\partial z} + \frac{1}{r} \frac{\partial u_z}{\partial \theta}, \gamma_{zr} = \frac{\partial u_r}{\partial z} + \frac{\partial u_z}{\partial r}, \\ \gamma_{r\theta} &= \frac{1}{r} \frac{\partial u_r}{\partial \theta} + \frac{\partial u_\theta}{\partial r} - \frac{u_\theta}{r} \end{aligned} \tag{17}$$

where u_r, u_θ and u_z are radial, circumferential and axial displacement components, respectively. Upon substitution Eq. (17) into (15) and then into (16), the equations of motion in terms of displacement components with infinitesimal deformations can be written as (Sobhani Aragh and Yas 2010):

$$\begin{bmatrix} K_{1r} & K_{1\theta} & K_{1z} \\ K_{2r} & K_{2\theta} & K_{2z} \\ K_{3r} & K_{3\theta} & K_{3z} \end{bmatrix} \begin{Bmatrix} u_r \\ u_\theta \\ u_z \end{Bmatrix} = \begin{Bmatrix} \rho \ddot{u}_r \\ \rho \ddot{u}_\theta \\ \rho \ddot{u}_z \end{Bmatrix} \tag{18}$$

The boundary conditions at the concave and convex surfaces, $r=r_i$ and r_o , respectively, can be described as follows:

-For $r=r_i$

$$\tau_{rz} = \tau_{r\theta} = \sigma_r = 0 \tag{19}$$

-For $r=r_o$

$$\tau_{rz} = \tau_{r\theta} = 0, \sigma_r = k_w u_r - k_g \Delta u_r \tag{20}$$

where $\Delta = \frac{\partial^2}{\partial z^2} + \left(\frac{1}{r^2}\right) \frac{\partial^2}{\partial \theta^2}$

We seek a semi-inverse solution for the displacement field for simply supported edges at $z=0$ and L by assuming that (Sobhani Aragh and Yas 2010):

$$\begin{aligned}
 u_r(r, \theta, z) &= \sum_{m=1}^{\infty} \sum_{n=1}^{\infty} U_r(r) \sin(m\theta) \sin(p_n z) e^{i\omega t}, \\
 u_\theta(r, \theta, z) &= \sum_{m=1}^{\infty} \sum_{n=1}^{\infty} U_\theta(r) \cos(m\theta) \sin(p_n z) e^{i\omega t}, \quad (21) \\
 u_z(r, \theta, z) &= \sum_{m=1}^{\infty} \sum_{n=1}^{\infty} U_z(r) \sin(m\theta) \cos(p_n z) e^{i\omega t}
 \end{aligned}$$

where $p_n = \frac{n\pi}{L}$. Also, “m” and “n” are circumferential and axial wave numbers, respectively, and ω is the natural angular frequency of the vibration. The simply supported opposite edges at $z=0$ and L are identically satisfied by the assumed displacement field.

3. Solution procedure

3.1 DQM solution for equations of motion and boundary conditions

It is necessary to develop appropriate methods to investigate the mechanical responses of sandwich structures. But, due to the complexity of the problem, it is difficult to obtain the exact solution. In this paper, the differential quadrature method (DQM) approach is used to solve the governing equations of sandwich curved panel. One can compare the DQM solution procedure with the other two widely used traditional methods for plate analysis, i.e., Rayleigh-Ritz method and FEM. The main difference between the DQM and the other methods is how the governing equations are discretized. In DQM the governing equations and boundary conditions are directly discretized, and thus elements of stiffness and mass matrices are evaluated directly. But in Rayleigh-Ritz and FEMs, the weak form of the governing equations should be developed and the boundary conditions are satisfied in the weak form. Generally by doing so larger number of integrals with increasing amount of differentiation should be done to arrive at the element matrices. Also, the number of degrees of freedom will be increased for an acceptable accuracy.

In Generalized Differential Quadrature Method (GDQM), the n th order partial derivative of a continuous function $f(x, z)$ with respect to x at a given point x_i can be approximated as a linear summation of weighted function values at all the discrete points in the domain of x , that is

$$\frac{\partial^n f(x_i, z)}{\partial x^n} = \sum_{k=1}^N q_{ik}^n f(x_k, z) \quad (i = 1, 2, \dots, N, n = 1, 2, \dots, N - 1) \quad (22)$$

where N is the number of sampling points and q_{ij}^n is the x dependent weight coefficient. To determine the weighting coefficients q_{ij}^n , the Lagrange interpolation basic functions are used as the test functions, and explicit formulas for computing these weighting coefficients can be obtained as

(Shu 2000)

$$q_{ij}^{(1)} = \frac{M^{(1)}(x_i)}{(x_i - x_j)M^{(1)}(x_j)}, \quad i, j = 1, 2, \dots, N, i \neq j \quad (23)$$

where

$$M^{(1)}(x_i) = \prod_{j=1, i \neq j}^N (x_i - x_j) \quad (24)$$

and for higher order derivatives, one can use the following relations iteratively

$$q_{ij}^{(n)} = n(q_{ii}^{(n-1)} q_{ij}^1 - \frac{q_{ij}^{(n-1)}}{(x_i - x_j)}), \quad i, j = 1, 2, \dots, N, \quad (25)$$

$$i \neq j, n = 2, 3, \dots, N - 1$$

$$q_{ii}^{(n)} = - \sum_{j=1, i \neq j}^N q_{ij}^{(n)} \quad i = 1, 2, \dots, N, \quad n = 1, 2, \dots, N - 1 \quad (26)$$

A simple and natural choice of the grid distribution is the uniform grid-spacing rule. However, it was found that non-uniform grid-spacing yields result with better accuracy. Hence, in this work, the Chebyshev-Gauss-Lobatto quadrature points are used

$$x_i = \frac{1}{2} (1 - \cos(\frac{i-1}{N-1} \pi)) \quad i = 1, 2, \dots, N \quad (27)$$

3.2 Discretization procedure

By applying Eq. 22 to Eq. 18 and by using the considered displacement field (Eq. 21), the discretized equations take the following forms

$$\begin{aligned}
 & -C_{55} p_n \sum_{k=1}^N c_{ik}^{(1)} U_{zk} - C_{55} p_n^2 U_{ri} + C_{44} \frac{m}{r^2} U_{\theta i} \\
 & -C_{44} \frac{m}{r} \sum_{k=1}^N c_{ik}^{(1)} U_{\theta k} - C_{44} \frac{m^2}{r^2} U_{ri} \\
 & + (\frac{\partial C_{23}}{\partial r}) \frac{1}{r} U_{ri} - C_{13} p_n \sum_{k=1}^N c_{ik}^{(1)} U_{zk} \\
 & -C_{23} \frac{m}{r} \sum_{k=1}^N c_{ik}^{(1)} U_{\theta k} - (\frac{\partial C_{23}}{\partial r}) \frac{m}{r} U_{\theta i} \\
 & + C_{33} \sum_{k=1}^N c_{ik}^{(2)} U_{rk} - C_{13} \frac{1}{r} p_n U_{zi} (\frac{\partial C_{33}}{\partial r} + \frac{C_{33}}{r}) \\
 & \sum_{k=1}^N c_{ik}^{(1)} U_{rk} + C_{12} \frac{1}{r} p_n U_{zi} \\
 & - (\frac{\partial C_{13}}{\partial r}) p_n U_{zi} - \frac{C_{22}}{r^2} U_{ri} \\
 & + C_{22} \frac{m}{r^2} U_{\theta i} = -\omega^2 \rho U_{ri}
 \end{aligned} \quad (28a)$$

$$\begin{aligned}
& C_{23} \frac{m}{r} \sum_{k=1}^N c_{ik}^{(1)} U_{rk} + C_{44} \sum_{k=1}^N c_{ik}^{(2)} U_{\theta k} \\
& + C_{44} \frac{m}{r} \sum_{k=1}^N c_{ik}^{(1)} U_{rk} \\
& + \left(\frac{\partial C_{44}}{\partial r} \right) \frac{m}{r} U_{ri} - C_{66} p_n^2 U_{\theta i} - C_{66} \frac{m}{r} p_n U_{zi} \\
& - C_{12} \frac{m}{r} p_n U_{zi} + C_{22} \frac{m}{r^2} U_{ri} - C_{22} \frac{m^2}{r^2} U_{\theta i} \\
& - \frac{1}{r} \left(\frac{\partial C_{44}}{\partial r} \right) U_{\theta i} - C_{44} \frac{1}{r^2} U_{\theta i} + \left(\frac{\partial C_{44}}{\partial r} + \frac{C_{44}}{r} \right) \\
& \sum_{k=1}^N c_{ik}^{(1)} U_{\theta k} + C_{44} \frac{m}{r^2} U_{ri} = -\omega^2 \rho U_{\theta i}
\end{aligned} \tag{28b}$$

$$\begin{aligned}
& -C_{11} p_n^2 U_{zi} + \left(\frac{\partial C_{55}}{\partial r} \right) p_n U_{ri} + C_{12} \frac{1}{r} p_n U_{ri} \\
& - C_{12} \frac{m}{r} p_n U_{\theta i} + C_{13} p_n \sum_{k=1}^N c_{ik}^{(1)} U_{rk} - \\
& C_{66} \frac{m}{r} p_n U_{\theta i} - C_{66} \frac{m^2}{r^2} U_{zi} + \\
& C_{55} \sum_{k=1}^N c_{ik}^{(2)} U_{zk} + C_{55} p_n \sum_{k=1}^N c_{ik}^{(1)} U_{rk} + \\
& \left(\frac{C_{55}}{r} + \frac{\partial C_{55}}{\partial r} \right) \sum_{k=1}^N c_{ik}^{(1)} U_{zk} + \\
& \frac{C_{55}}{r} p_n U_{ri} = -\omega^2 \rho U_{zi}
\end{aligned} \tag{28c}$$

In the above equation, $C_{ik}^{(1)}$ and $C_{ik}^{(2)}$ are the weighting coefficients of the first and second-order derivatives. The discretized forms of boundary conditions on the inner and outer surfaces of the cylindrical shell, shown in equation (19), can be expressed as follows:

-On the inner surface ($r=r_i$):

$$\begin{aligned}
& C_{23}^1 \frac{1}{r_i} U_{r1} + C_{33}^1 c_{11}^{(1)} U_{r1} + C_{33}^1 c_{1N}^{(1)} U_{rN} - \\
& C_{23}^1 \frac{m}{r_i} U_{\theta 1} - C_{13}^1 p_n U_{z1} + C_{33}^1 \sum_{k=2}^{N-1} c_{1k}^{(1)} U_{rk} = 0, \\
& C_{44}^1 \frac{m}{r_i} U_{r1} - C_{44}^1 \frac{1}{r_i} U_{\theta 1} + C_{44}^1 c_{11}^{(1)} U_{\theta 1} + \\
& C_{44}^1 c_{1N}^{(1)} U_{\theta N} + C_{44}^1 \sum_{k=2}^{N-1} c_{1k}^{(1)} U_{\theta k} = 0, \\
& C_{55}^1 c_{11}^{(1)} U_{z1} + C_{55}^1 \sum_{k=2}^{N-1} c_{1k}^{(1)} U_{zk} + \\
& C_{55}^1 c_{1N}^{(1)} U_{zN} + C_{55}^1 p_n U_{r1} = 0
\end{aligned} \tag{29}$$

-On the outer surface ($r=r_o$):

$$\begin{aligned}
& C_{33}^N c_{N1}^{(1)} U_{r1} + C_{23}^N \frac{1}{r_o} U_{rN} + C_{33}^N c_{NN}^{(1)} U_{rN} - \\
& C_{23}^N \frac{m}{r_o} U_{\theta N} - C_{13}^N p_n U_{zN} + C_{33}^N \sum_{k=2}^{N-1} c_{Nk}^{(1)} U_{rk} + \\
& \left\{ k_w + k_g p_n^2 + k_g m^2 \left(\frac{1}{r_o^2} \right) \right\} U_{rN} = 0,
\end{aligned} \tag{30}$$

$$\begin{aligned}
& C_{44}^N \frac{m}{r_o} U_{rN} - C_{44}^N \frac{1}{r_o} U_{\theta N} + C_{44}^N c_{N1}^{(1)} U_{\theta 1} + \\
& C_{44}^N c_{NN}^{(1)} U_{\theta N} + C_{44}^N \sum_{k=2}^{N-1} c_{Nk}^{(1)} U_{\theta k} = 0, \\
& C_{55}^N c_{N1}^{(1)} U_{z1} + C_{55}^N \sum_{k=2}^{N-1} c_{Nk}^{(1)} U_{zk} + \\
& C_{55}^N c_{NN}^{(1)} U_{zN} + C_{55}^N p_n U_{rN} = 0
\end{aligned}$$

Applying the GDQ procedure, the whole system of differential equations has been discretized and the global assembling leads to the following set of linear algebraic equations

$$\begin{Bmatrix} [A_{bb}] & [A_{bd}] \\ [A_{db}] & [A_{dd}] \end{Bmatrix} \begin{Bmatrix} \{U_b\} \\ \{U_d\} \end{Bmatrix} = \begin{Bmatrix} \{0\} \\ -\omega^2 [M] \{U_d\} \end{Bmatrix} \tag{31}$$

In the above relations, subscripts b and d correspond to the displacement vectors at boundaries and domain of the shell, respectively. The natural frequencies of the considered cylindrical shells can be determined by solving the standard eigenvalue problem.

4. Numerical results and discussion

To verify the proficiency of presented method several numerical examples are carried out for comparisons. It is mentioned that the accurate results in the following tables are obtained for $N=13$. The obtained natural frequencies based on the three-dimensional elasticity formulation are compared with the results reported by Wang and Liu (2019), Beni *et al.* (2016) and Alibeigloo and Shaban (2013) as shown in Table 3. As observed, there is a good agreement between the results.

Further validation of the present results for an FG cylindrical shell is shown in Table 4. The comparisons show that the present results agreed well with those in the literature. After demonstrating the convergence and accuracy of the present method, natural frequencies of sandwich cylindrical shell with damaged core and FG face sheets based on the three-dimensional theory of elasticity are computed. The non-dimensional natural frequency can be assumed as follows:

$$\begin{aligned}
\Omega &= \omega h \sqrt{\frac{\rho_i}{E_i}}, K_g = 100 * k_g \frac{H^2}{D_i}, \\
K_w &= 100 * k_w \frac{H^4}{D_i}, D_i = E_i \frac{H^3}{12(1 - \nu_i^2)}
\end{aligned} \tag{32}$$

where ρ_i , E_i and ν_i are mechanical properties of CNT.

From the results depicted in Fig. 6, one can see that the natural frequency of each material distribution depends on the parameter D. Due to stiffness reduction of the structures, the frequency of sandwich cylindrical shell decreases. It should be noted that by increasing the value of D up to the unity (fully damaged core) the frequency would tend to become zero.

The influence of the index P on the natural frequency is shown in Figs. 7 and 8. It should be noticed that with increase of volume fraction of fibers, the frequency

Table 3 Comparison of dimensionless natural frequency of the isotropic homogeneous S-S cylindrical shell

H/R	n	Present	Wang and Liu (2019)	Beni <i>et al.</i> (2016)	Alibeigloo and Shaban (2013)
1	0.1954	0.1959	0.1959	0.2004	
0.05	2	0.2620	0.2623	0.2623	0.2633
	3	0.3222	0.3220	0.3220	0.3158
1	0.1952	0.1954	0.1954	0.1968	
0.02	2	0.2535	0.2532	0.2532	0.2563
	3	0.2772	0.2772	0.2772	0.2773

parameter of the panels does not increase necessarily, so by

Table 4 Comparison of natural frequency of the S-S functionally graded cylindrical shell

N	Present	Loy <i>et al.</i> (1999)	Liu <i>et al.</i> (2018)	Wang and Liu (2019)
1	13.221	13.211	13.242	13.229
2	4.621	4.480	4.480	4.624
3	4.5524	4.1569	4.1459	4.5502
4	7.4780	7.0384	7.0325	7.4799
5	11.689	11.241	11.229	11.684
6	16.914	16.455	16.438	16.891
7	23.055	22.635	22.612	23.060
8	30.181	29.771	29.741	30.183
9	38.221	37.862	37.822	38.257
10	47.271	46.905	46.855	47.283

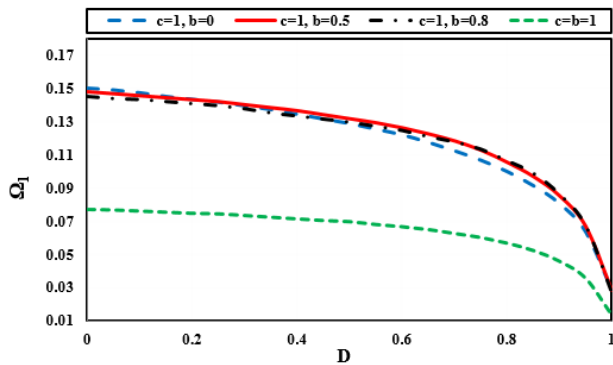


Fig. 6 Variation of the natural frequency for the sandwich cylindrical shell versus parameter D ($P=2, K_w=100, K_g=10, V_F^*=0.12$)

considering suitable amounts of power-law index P ($0 \leq P \leq \infty$) and the parameters b and c , one can get dynamic characteristics similar or better than the isotropic limit case for laminated FG structures. Fig. 9 shows that for $P>3$ and ($0 \leq b \leq 1$), the discrepancy between natural frequencies of the FG sandwich shells, increase with the increase of P . For $P<1$ and ($0 \leq b \leq 1$), increasing of parameter b does not have significant effect on the discrepancy amount of natural frequency parameters of the FG sandwich shell. As can be seen from Fig. 8, with the increase of P , the discrepancy between the natural frequencies of the shells for different amounts of parameter c sharply decreases.

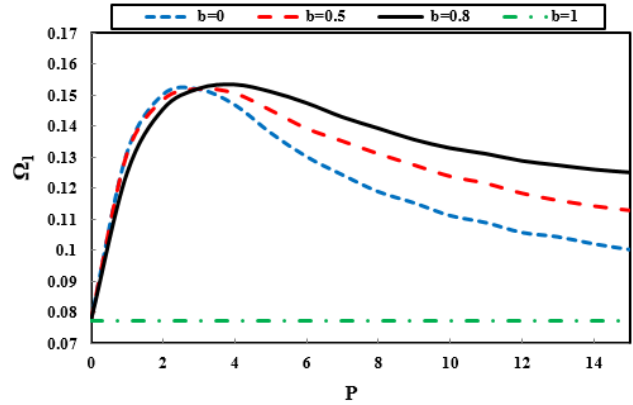


Fig. 7 The first non-dimensional natural frequency of the FG sandwich cylindrical shell versus p for different amounts of b ($D=0, K_w=100, K_g=10, V_F^*=0.12$)

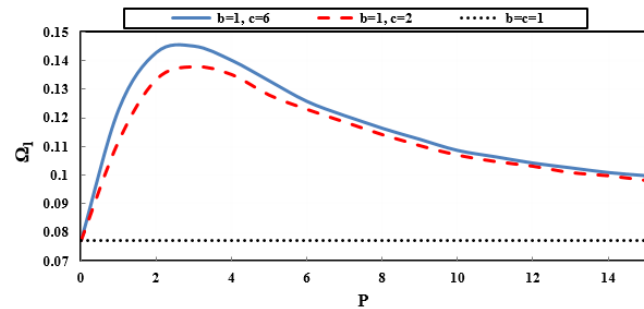


Fig. 8 The first non-dimensional natural frequency of the FG sandwich shells versus P for different amounts of coefficient ($D=0, V_F^*=0.12, K_w=100, K_g=10$)

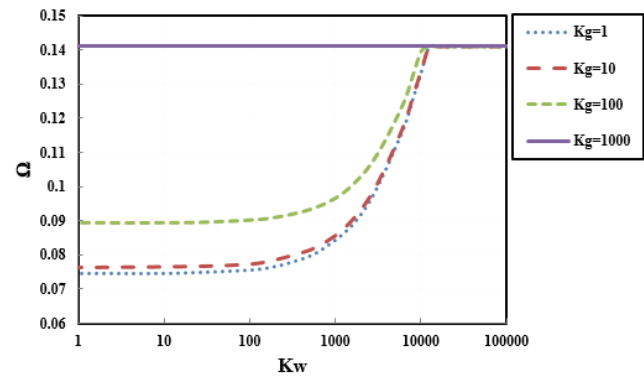


Fig. 9 Variation of the first nondimensional natural frequency of FGS cylindrical shell resting on an elastic foundation versus Winkler elastic coefficient for different shearing layer elastic coefficients ($D=0, V_F^*=0.12, P=2, b=c=1$)

The effects of the elastic foundation coefficients (K_w and K_g) on the first nondimensional natural frequencies of FGS cylindrical shells are shown in Figs. 9 and 10. As observed from these figures, both Winkler and shearing layer elastic coefficients have significant effects on the frequencies of FGS shell. Fig. 9 shows the effect of Winkler elastic coefficient on the first natural frequency parameter for different values of shearing layer elastic coefficients. It is seen that the most effective range of Winkler foundation

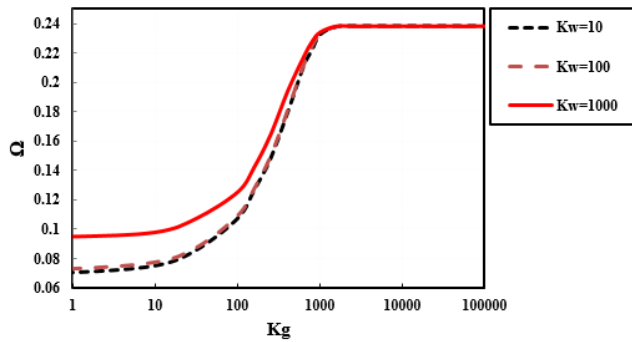


Fig. 10 Variation of the first nondimensional natural frequency of FGS cylindrical shell resting on an elastic foundation versus shearing layer elastic coefficients for different Winkler elastic coefficient ($D=0$, $V_F^*=0.12$, $P=2$, $b=c=1$)

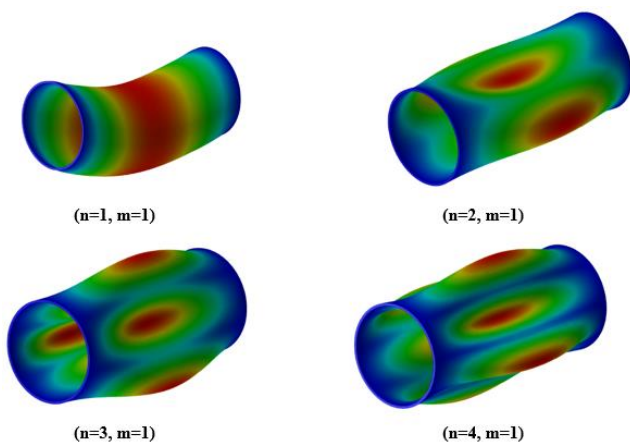


Fig. 11 The modal shapes of a laminated cylindrical shell with simply-supported (S-S) boundary conditions

stiffness in increasing the natural frequency is from 10^0 to 10^4 . It is also observed for the large values of Winkler elastic coefficient, the shearing layer elastic coefficient has less effect and the results become independent of it. In other words, the natural frequencies converge with increasing Winkler foundation stiffness. The influence of shearing layer elastic coefficients on the first nondimensional natural frequency is shown in Fig. 10. The most effective range of shearing layer foundation stiffness in increasing the non-dimensional natural frequency is from 100 to 103. It shows that the variation of Winkler elastic coefficient does not have any effect on the nondimensional natural frequency for $K_g > 10^3$. Figs. 9 and 10 yield a good insight to designers because these figures indicate that the foundation stiffness should be considered in the special effective ranges.

In order to further investigate the free vibration characteristics of composite laminated cylindrical shells with simply supported-simply supported (S-S) boundary conditions, some mode shapes (n,m) of the composite laminated cylindrical shell are shown in Fig. 11.

5. Conclusions

This research work presents vibration analysis of

sandwich cylindrical shell resting on a two-parameter elastic foundation with damaged core and FG face sheets based on the three-dimensional theory of elasticity. The core of the sandwich structures considered in the paper is made of the same polymer matrix used in the face-sheets. A damage model is introduced to provide an analytical description of an irreversible rheological process that causes the decay of the mechanical properties, in terms of engineering constants. An isotropic damage is considered for the core of the sandwich cylindrical shell. Three complicated equations of motion for the curved panel under consideration are semi-analytically solved by generalized differential quadrature (GDQ) method. Using the GDQ method, allows one to implement the effects of the elastic foundations as a boundary condition on the outer surface of the sandwich cylindrical shell and in exact manner. Several parametric analyses are carried out to investigate the mechanical behavior of these multi-layered structures depending on the damage features. From this study, some conclusions can be made:

- It is also seen that for large amount of parameter “P”, increasing this parameter does not have significant effect on the non-dimensional natural frequency parameters of FG sandwich cylindrical shell.

- It should be noted that by increasing the value of D up to the unity (fully damaged core) the frequency would tend to become zero.

- It is observed that with increase of volume fraction of fibers, the frequency parameter of the panels does not increase necessarily, so by considering suitable amounts of power-law index P ($0 \leq P \leq \infty$) and the parameters b and c , one can get dynamic characteristics similar or better than the isotropic limit case for laminated FG cylindrical shell.

- It is also observed for the large values of Winkler elastic coefficient, the shearing layer elastic coefficient has less effect and the results become independent of it.

- The most effective range of shearing layer foundation stiffness in increasing the nondimensional natural frequency is from 1 to 10^3 . It shows that the variation of Winkler elastic coefficient does not have any effect on the nondimensional natural frequency for $K_g > 10^3$.

These comments should be taken into account during the analysis of the mechanical behavior of sandwich structures subjected to a progressive damage, as well as during the process manufacturing if an optimal design has to be pursued.

Acknowledgment

This study is supported via funding from Prince Satam bin Abdulaziz University project number (PSAU/2024/R/1446)

References

- Abouelregal, A.E. and Marin, M. (2020a), “The response of nanobeams with temperature-dependent properties using state-space method via modified couple stress theory”, *Symmetry*, **12**(8), 1276. <https://doi.org/10.3390/sym12081276>.
- Abouelregal, A.E. and Marin, M. (2020b), “The size-dependent

- thermoelastic vibrations of nanobeams subjected to harmonic excitation and rectified sine wave heating”, *Mathematics*, **8**(7). <https://doi.org/10.3390/math8071128>.
- Abrate, S. (1998), *Impact on Composite Structures*, Cambridge University Press, Cambridge, U.K.
- Affdl Halpin, J.C. and Kardos, J.L. (1976), “The Halpin-Tsai equations: A review”, *Polym. Eng. Sci.*, **16**(5), 344-352. <https://doi.org/10.1002/pen.760160512>.
- Afrokhteh, S.S., Fathi, A., Naghdipour, M. and Alizadeh Sahraei, A. (2016), “An experimental investigation of the effects of weight fractions of reinforcement and timing of hardener addition on the strain sensitivity of carbon nanotube/polymer composites”, *U.P.B. Sci. Bull., Series B*, **78**(4), 121-130.
- Afrokhteh, S.S., Shakeri, M., Baniassadi, M. and Alizadeh Sahraei, A. (2018), “Microstructure reconstruction and characterization of the porous GDLs for PEMFC based on fibers orientation distribution”, *Fuel Cells*, **18**(2). <https://doi.org/10.1002/fuce.201700239>.
- Alibeigloo, A. and Shaban, M. (2013), “Free vibration analysis of carbon nanotubes by using three-dimensional theory of elasticity”, *Acta Mech*, **224**, 1415-1427. <https://doi.org/10.1007/s00707-013-0817-2>
- Amari, A., Mohammed, B.A., Salman, H.M. and Lagos, J.M. (2023), “Numerical assessment of the nanocomposite sector annular plates with the aim of promoting their mixed-form thermal shock response”, *Eng. Anal. Bound. Elem.*, **146**, 483-499. <https://doi.org/10.1016/j.enganabound.2022.10.031>.
- Anderson, T.A. (2003), “3D elasticity solution for a sandwich composite with functionally graded core subjected to transverse loading by a rigid sphere”, *Compos. Struct.*, **60**(3), 265-274. [https://doi.org/10.1016/S0263-8223\(03\)00013-8](https://doi.org/10.1016/S0263-8223(03)00013-8).
- Arefi, M. (2015), “Elastic solution of a curved beam made of functionally graded materials with different cross sections”, *Steel Compos. Struct.*, **18**(3), 659-672. <https://doi.org/10.12989/scs.2015.18.3.659>.
- Baccocchi, M., Tarantino, A.M. (2019), “Time-dependent behavior of viscoelastic three-phase composite plates reinforced by carbon nanotubes”, *Compos. Struct.*, **216**, 20-31. <https://doi.org/10.1016/j.compstruct.2019.02.083>.
- Barka, M., Benrahou, K.H., Bakora, A. and Tounsi, A. (2016), “Thermal post-buckling behavior of imperfect temperature-dependent sandwich FGM plates resting on Pasternak elastic foundation”, *Steel Compos. Struct.*, **22**(1), 91-112. <https://doi.org/10.12989/scs.2016.22.1.091>.
- Bellman, R. and Casti, J. (1971), “Differential quadrature and long term integration”, *J. Math. Anal. Appl.*, **34**(2), 235-238. [https://doi.org/10.1016/0022-247X\(71\)90110-7](https://doi.org/10.1016/0022-247X(71)90110-7).
- Beni, Y.T., Mehralian, F. and Zeighampour, H. (2016), “The modified couple stress functionally graded cylindrical thin shell formulation”, *Mech. Adv. Mater. Struct.*, **23**(7), 791-801. <http://doi.org/10.1080/15376494.2015.1029167>.
- Bennai, R., Ait Atmane, H. and Tounsi, A. (2015), “A new higher-order shear and normal deformation theory for functionally graded sandwich beams”, *Steel Compos. Struct.*, **19**(3), 521-546. <https://doi.org/10.12989/scs.2015.19.3.521>.
- Bouchafa, A., Bouiadjra, M.B., Houari, M.S.A. and Tounsi, A. (2015), “Thermal stresses and deflections of functionally graded sandwich plates using a new refined hyperbolic shear deformation theory”, *Steel Compos. Struct.*, **18**(6), 1493-1515. <https://doi.org/10.12989/scs.2015.18.6.1493>.
- Bouafia, H., Chikh, A., Bousahla, A.A., Bourada, F., Heireche, H., Tounsi, A., Benrahou, K.H., Tounsi, A., Al-Zahrani, M.M. and Hussain, M. (2021), “Natural frequencies of FGM nanoplates embedded in an elastic medium”, *Adv. Nano Res.*, **11**(3), 239-249. <https://doi.org/10.12989/anr.2021.11.3.239>.
- Bouguenina, O., Belakhdar, K., Tounsi, A. and Bedia, E.A.A. (2015), “Numerical analysis of FGM plates with variable thickness subjected to thermal buckling”, *Steel Compos. Struct.*, **19**(3), 679-695. <https://doi.org/10.12989/scs.2015.19.3.679>.
- Boutaleb, S., Benrahou, K.H., Bakora, A., Algarni, A., Bousahla, A.A., Tounsi, A., Tounsi, A. and Mahmoud, S.R. (2019), “Dynamic analysis of nanosize FG rectangular plates based on simple nonlocal quasi 3D HSDT”, *Adv. Nano Res.* **7**(3), 191-208. <https://doi.org/10.12989/anr.2019.7.3.191>.
- Brischetto, S., Tornabene, F., Fantuzzi, N. and Baccocchi, M. (2015), “Refined 2D and exact 3D shell models for the free vibration analysis of single- and double-walled carbon nanotubes”, *Technologies*, **3**(4), 259-284. <https://doi.org/10.3390/technologies3040259>.
- Chen, C.S., Liu, F.H. and Chen, W.R. (2017), “vibration and stability of initially stressed sandwich plates with FGM face sheets in thermal environments”, *Steel Compos. Struct.*, **23**(3), 251-261. <https://doi.org/10.12989/scs.2017.23.3.251>.
- Chen, W.Q., Bian, Z.G. and Ding, H.U. (2004), “Three-dimensional vibration analysis of fluid-filled orthotropic FGM cylindrical shells”, *Int. J. Mech. Sci.*, **46**(1), 159-171. <https://doi.org/10.1016/j.ijmecsci.2003.12.005>.
- Civalek, Ö. (2005), “Geometrically nonlinear dynamic analysis of doubly curved isotropic shells resting on elastic foundation by a combination of HDQ-FD methods”, *Int. J. Press Vessel Pip.*, **82**(6), 470-479. <https://doi.org/10.1016/j.ijpvp.2004.12.003>.
- Dai, Z., Jiang, Z., Zhang, L. and Habibi, M. (2021), “Frequency characteristics and sensitivity analysis of a size-dependent laminated nanoshell”, *Adv. Nano Res.*, **10**(2), 175-189. <https://doi.org/10.12989/anr.2021.10.2.175>.
- Ebrahimi, F., Fardshad, R.E. and Mahesh, V. (2019), “Frequency response analysis of curved embedded magneto-electro-viscoelastic functionally graded nanobeams”, *Adv. Nano Res.*, **7**(6), 391-403. <https://doi.org/10.12989/anr.2019.7.6.391>.
- Eshelby, J.D. (1957), “The determination of the elastic field of an ellipsoidal inclusion, and related problems”, *P. Roy. Soc. Lond. A Mat.*, **241**, 376-396. <https://www.jstor.org/stable/100095>.
- Fantuzzi, N., Tornabene, F., Baccocchi, M. and Dimitri, R. (2016), “Free vibration analysis of arbitrarily shaped functionally carbon nanotube-reinforced plates”, *Compos. Part B*, **115**(1), 384-408. <https://doi.org/10.1016/j.compositesb.2016.09.021>.
- Gang, S.W., Lam, K.Y. and Reddy, J.N. (1999), “The elastic response of functionally graded cylindrical shells to low-velocity”, *Int. J. Impact Eng.*, **22**(4), 397-417. [https://doi.org/10.1016/S0734-743X\(98\)00058-X](https://doi.org/10.1016/S0734-743X(98)00058-X).
- Ghavamian, A., Rahmandoust, M. and Öchsner, A. (2012), “A numerical evaluation of the influence of defects on the elastic modulus of single and multi-walled carbon nanotubes”, *Comput. Mater. Sci.*, **62**, 110-116. <https://doi.org/10.1016/j.commatsci.2012.05.003>.
- Halpin, J.C. and Tsai, S.W. (1969), “Effects of environmental factors on composite materials”, AFML-TR-67-423.
- Hill, R. (1964a), “Theory of mechanical properties of fibre-strengthened materials Elastic behavior”, *J. Mech. Phys. Solids*, **12**, 199-212. [https://doi.org/10.1016/0022-5096\(64\)90019-5](https://doi.org/10.1016/0022-5096(64)90019-5).
- Hill, R. (1964b), “Theory of mechanical properties of fibre-strengthened materials: II. Inelastic behavior”, *J. Mech. Phys. Solids*, **12**, 213-218. [https://doi.org/10.1016/0022-5096\(64\)90020-1](https://doi.org/10.1016/0022-5096(64)90020-1).
- Hong, M. and Lee, U. (2015), “Dynamics of a functionally graded material axial bar, Spectral element modeling and analysis”, *Compos. Part B*, **69**, 427-434. <https://doi.org/10.1016/j.compositesb.2014.10.022>.
- Hosseini, S.M. and Zhang, C. (2018), “Elastodynamic and wave propagation analysis in a FG Graphene platelets-reinforced nanocomposite cylinder using a modified nonlinear micro-mechanical model”, *Steel Compos. Struct.*, **27**(3), 255-271. <https://doi.org/10.12989/scs.2018.27.3.255>
- Jam, J.E., Noorabadi, M. and Namdaran, N. (2017), “Nonlinear

- free vibration analysis of micro-beams resting on viscoelastic foundation based on the modified couple stress theory”, *Arch. Mech. Eng.*, **64**(2). <https://doi.org/10.1515/meceng-2017-0015>.
- Kamarian, S., Yas, M.H. and Poursasghar, A. (2013), “Free vibration analysis of three-parameter functionally graded material sandwich plates resting on Pasternak foundations”, *Sandw. Struct. Mater.*, **15**(3) 292-308. <https://doi.org/10.1177/1099636213487363>.
- Kashtalyan, M. and Menshykova, M. (2009), “Three-dimensional elasticity solution for sandwich panels with a functionally graded core”, *Compos. Struct.*, **87**(1), 36-43. <https://doi.org/10.1016/j.compstruct.2007.12.003>.
- Khadir, A.I., Daikh, A.A. and Eltaher, M.A. (2021), “Novel four-unknowns quasi 3D theory for bending, buckling and free vibration of functionally graded carbon nanotubes reinforced composite laminated nanoplates”, *Adv. Nano Res.*, **11**(6), 621-640. <https://doi.org/10.12989/anr.2021.11.6.621>.
- Lemaitre, J., Chaboche, J.L. (1990), *Mechanics of Solid Materials*, Cambridge University Press, New York, N.Y., U.S.A.
- Li, Q., Iu, V.P. and Kou, K.P. (2008), “Three-dimensional vibration analysis of functionally graded material sandwich plates”, *J. Sound Vib.*, **311**(1-2), 498-515. <https://doi.org/10.1016/j.jsv.2007.09.018>.
- Liu, D., Kitipornchai, S., Chen, W. and Yang, J. (2018), “Three-dimensional buckling and free vibration analyses of initially stressed functionally graded graphene reinforced composite cylindrical shell”, *Compos. Struct.*, **189**, 560-569. <https://doi.org/10.1016/j.compstruct.2018.01.106>.
- Loy, C.T., Lam, K.Y. and Reddy, J.N. (1999), “Vibration of functionally graded cylindrical shells”, *Int. J. Mech. Sci.*, **41**(3), 309-324. [https://doi.org/10.1016/S0020-7403\(98\)00054-X](https://doi.org/10.1016/S0020-7403(98)00054-X)
- Marin, M. and Öchsner, A. (2017), “The effect of a dipolar structure on the Hölder stability in Green–Naghdi thermoelasticity”, *Continuum Mech. Thermodyn.*, **29**(6), 1365-1374. <https://doi.org/10.1007/s00161-017-0585-7>.
- Matsunaga, H. (2008), “Free vibration and stability of functionally graded shallow shells according to a 2-D higher-order deformation theory”, *Compos. Struct.*, **84**(2), 132-146. <https://doi.org/10.1016/j.compstruct.2007.07.006>.
- Moradi-Dastjerdi, R. and Momeni-Khabisi, H. (2016), “Dynamic analysis of functionally graded nanocomposite plates reinforced by wavy carbon nanotube”, *Steel Compos. Struct.*, **22**(2), 277-299. <https://doi.org/10.12989/scs.2016.22.2.277>.
- Mori, T. and Tanaka, K. (1973), “Average stress in matrix and average elastic energy of materials with misfitting inclusions”, *Acta Metall.*, **21**, 571-574. [https://doi.org/10.1016/0001-6160\(73\)90064-3](https://doi.org/10.1016/0001-6160(73)90064-3).
- Odegard, G.M., Gates, T.S., Wise, K.E., Park, C. and Siochi, E.J. (2003), “Constitutive modeling of nanotube-reinforced polymer composites”, *Compos. Sci. Technol.*, **63**, 1671-1687. [https://doi.org/10.1016/S0266-3538\(03\)00063-0](https://doi.org/10.1016/S0266-3538(03)00063-0).
- Othman, M.I.A. and Marin, M. (2017), “Effect of thermal loading due to laser pulse on thermoelastic porous medium under GN theory”, *Results Phys.*, **7**, 3863-3872. <https://doi.org/10.1016/j.rinp.2017.10.012>.
- Paliwal, D.N., Kanagasabapathy, H. and Gupta, K.M. (1995), “The large deflection of an orthotropic cylindrical shell on a Pasternak foundation”, *Compos. Struct.*, **31**, 31-37. [https://doi.org/10.1016/0263-8223\(94\)00068-9](https://doi.org/10.1016/0263-8223(94)00068-9).
- Paliwal, D.N., Pandey, R.K. and Nath, T. (1996), “Free vibration of circular cylindrical shell on Winkler and Pasternak foundation”, *Int. J. Press. Vessel Pip.*, **69**(1), 79-89. [https://doi.org/10.1016/0308-0161\(95\)00010-0](https://doi.org/10.1016/0308-0161(95)00010-0).
- Park, W.T., Han, S.C., Jung, W.Y. and Lee, W.H. (2016), “Dynamic instability analysis for S-FGM plates embedded in Pasternak elastic medium using the modified couple stress theory”, *Steel Compos. Struct.*, **22**(6), 1239-1259. <https://doi.org/10.12989/scs.2016.22.6.1239>.
- Patel, B.P., Gupta, S.S., Loknath, M.S.B. and Kadu, C.P. (2005), “Free vibration analysis of functionally graded elliptical cylindrical shells using higher-order theory”, *Compos. Struct.*, **69**(3), 259-270. <https://doi.org/10.1016/j.compstruct.2004.07.002>.
- Pelletier Jacob, L. and Vel Senthil, S. (2006), “An exact solution for the steady state thermo elastic response of functionally graded orthotropic cylindrical shells”, *Int. J. Solid Struct.*, **43**(5), 1131-1158. <https://doi.org/10.1016/j.ijsolstr.2005.03.079>.
- Pradhan, S.C., Loy, C.T., Lam, K.Y., Reddy, J.N. (2000), “Vibration characteristic of functionally graded cylindrical shells under various boundary conditions”, *Appl. Acoust.*, **61**(1), 119-129. [https://doi.org/10.1016/S0003-682X\(99\)00063-8](https://doi.org/10.1016/S0003-682X(99)00063-8).
- Pradyumna, S. and Bandyopadhyay, J.N. (2008), “Free vibration analysis of functionally graded panels using higher-order finite-element formulation”, *J. Sound Vib.*, **318**(1-2), 176-192. <https://doi.org/10.1016/j.jsv.2008.03.056>.
- Shakeri, M., Akhlaghi, M. and Hosseini, S.M. (2006), Vibration and radial wave propagation velocity in functionally graded thick hollow cylinder”, *J. Compos. Struct.*, **76**(1), 174-181. <https://doi.org/10.1016/j.compstruct.2006.06.022>.
- Shi, D.L., Huang, Y.Y., Hwang, K.C. and Gao, H. (2004), “The effect of nanotube waviness and agglomeration on the elastic property of carbon nanotube–reinforced composites”, *J. Eng. Mater. T. ASME*, **126**, 250-257. <https://doi.org/10.1115/1.1751182>.
- Shu, C. (2000), *Differential Quadrature and Its Application in Engineering*, Springer, Berlin.
- Sobhani Aragh, B. and Yas, M.H. (2010), “Static and free vibration analyses of continuously graded fiber-reinforced cylindrical shells using generalized power-law distribution”, *Acta Mech.*, **215**, 155-173. <https://doi.org/10.1007/s00707-010-0335-4>.
- Tahouneh, V. (2014), “Free vibration analysis of bidirectional functionally graded annular plates resting on elastic foundations using differential quadrature method”, *Struct. Eng. Mech.*, **52**(4), 663-686. <https://doi.org/10.12989/sem.2014.52.4.663>.
- Tahouneh, V., Naei, M.H. and Mosavi Mashhadi, M. (2020a), “Influence of vacancy defects on vibration analysis of graphene sheets applying isogeometric method: Molecular and continuum approaches”, *Steel Compos. Struct.*, **34**(2), 261-277. <http://doi.org/10.12989/scs.2020.34.2.261>.
- Tahouneh, V., Naei, M.H. and Mosavi Mashhadi, M. (2020b), “Using IGA and trimming approaches for vibrational analysis of L-shape graphene sheets via nonlocal elasticity theory”, *Steel Compos. Struct.*, **33**(5), 717-727. <http://doi.org/10.12989/scs.2019.33.5.717>.
- Tahouneh, V. (2016), “Using an equivalent continuum model for 3D dynamic analysis of nanocomposite plates”, *Steel Compos. Struct.*, **20**(3), 623-649. <https://doi.org/10.12989/scs.2016.20.3.623>.
- Tahouneh, V. and Naei, M.H. (2014), “A novel 2-D six-parameter power-law distribution for three-dimensional dynamic analysis of thick multi-directional functionally graded rectangular plates resting on a two-parameter elastic foundation”, *Meccanica*, **49**(1), 91-109. <https://doi.org/10.1007/s11012-013-9776-x>.
- Tornabene, F., Baccocchi, M., Fantuzzi, N. and Reddy, J.N. (2019), “Multiscale approach for three-phase cnt/polymer/fiber laminated nanocomposite structures”, *Polym. Compos.*, **40**, 102-126. <https://doi.org/10.1002/pc.24520>.
- Tornabene, F. (2009), “Free vibration analysis of functionally graded conical cylindrical shell and annular plate structures with a four-parameter power-law distribution”, *Comput. Meth. Appl. Mech. Eng.*, **198**(37), 2911-2935. <https://doi.org/10.1016/j.cma.2009.04.011>.
- Tornabene, F., Fantuzzi, N. and Baccocchi, M. (2014), “Free

- vibrations of free-form doubly curved shells made of functionally graded materials using higher-order equivalent single layer theories”, *Compos. Part B*, **67**(1), 490-509.
<https://doi.org/10.1016/j.compositesb.2014.08.012>.
- Tornabene, F., Fantuzzi, N., Baccocchi, M. and Viola, E. (2016a), “Effect of agglomeration on the natural frequencies of functionally graded carbon nanotube-reinforced laminated composite doubly-curved shells”, *Compos. Part B*, **89**(1), 187-218. <https://doi.org/10.1016/j.compositesb.2015.11.016>.
- Tornabene, F., Fantuzzi, N. and Baccocchi, M. (2016b), “Linear static response of nanocomposite plates and shells reinforced by agglomerated carbon nanotubes”, *Compos. Part B*, **115**(1), 449-476. <https://doi.org/10.1016/j.compositesb.2016.07.011>.
- Tsai, S.W. (1964), *Structural Behavior of Composite Materials*, Philco Corporation: Newport Beach, CA, U.S.A.
- Tsai, S.W. (1965), *Strength Characteristics of Composite Materials*, Philco Corporation: Newport Beach, CA, U.S.A.
- Vinson J.R. (2005), “Sandwich structures: past, present, and future. In: Proceedings of the 7th international conference on sandwich structures”, 3-12, Aalborg University, Aalborg, Denmark.
- Viola, E. and Tornabene, F. (2009), “Free vibrations of three-parameter functionally graded parabolic panels of revolution”, *Mech. Res. Commun.*, **36**(5), 587-594.
<https://doi.org/10.1016/j.mechrescom.2009.02.001>.
- Wagner, H.D., Lourie, O. and Feldman, Y. (1997), “Stress-induced fragmentation of multiwall carbon nanotubes in a polymer matrix”, *Appl. Phys. Lett.*, **72**(2), 188-190.
<https://doi.org/10.1063/1.120680>.
- Wang, L., Hu, H. (2014), “Thermal vibration single-walled carbon nanotubes with quantum effects”, *Proc. Math. Phys. Eng. Sci.*, **470**(2168). <https://doi.org/10.1098/rspa.2014.0087>.
- Wang, Y.Q. and Liu, Y.F. (2019), “Free vibration and buckling of polymeric shells reinforced with 3D graphene foams”, *Results Phys.*, **14**. <https://doi.org/10.1016/j.rinp.2019.102510>.
- Wu, C.P. and Liu, Y.C. (2016), “A state space meshless method for the 3D analysis of FGM axisymmetric circular plates”, *Steel Compos. Struct.*, **22**(1), 161-182.
<https://doi.org/10.12989/scs.2016.22.1.161>.
- Yang, J. and Shen, S.H. (2003), “Free vibration and parametric resonance of shear deformable functionally graded cylindrical panels”, *J. Sound Vib.*, **261**(5), 871-893.
[https://doi.org/10.1016/S0022-460X\(02\)01015-5](https://doi.org/10.1016/S0022-460X(02)01015-5).
- Yang, R., Kameda, H. and Takada, S. (1998), “Shell model FEM analysis of buried pipelines under seismic loading”, *Bull Disaster Prev Res. Inst.*, **38**, 115-146.
- Zenkour, A.M. (2005a), “A comprehensive analysis of functionally graded sandwich plates. Part 1-deflection and stresses”, *Int. J. Solid Struct.*, **42**(1), 5224-5242.
<https://doi.org/10.1016/j.ijsolstr.2005.02.015>.
- Zenkour, A.M. (2005b), “A comprehensive analysis of functionally graded sandwich plates. Part 1-buckling and free vibration deflection and stresses”, *Int. J. Solid Struct.*, **42**(18), 5243-5258.
<https://doi.org/10.1016/j.ijsolstr.2005.02.016>.
- Zhang, Y. and Wang L. (2020), “Effects of Van der Waals force on the vibration of typical Multi-layered Two-dimensional nanostructures”, *Sci. Rep.*, **10**(644).
<https://doi.org/10.1038/s41598-020-57522-9>.
- Zhang, L., Bhatti, M.M., Michaelides, E.E., Marin, M. and Ellahi, R. (2022), “Hybrid nanofluid flow towards an elastic surface with tantalum and nickel nanoparticles, under the influence of an induced magnetic field”, *Eur. Phys. J. Spec. Top.*, **231**, 521-533. <https://doi.org/10.1140/epjs/s11734-021-00409-1>